

## Structural Analysis of Carbyne Network Polymers

Scott A. Best, Patricia A. Bianconi,\* and Kenneth M. Merz, Jr.\*

Contribution from the Department of Chemistry, The Pennsylvania State University, University Park, Pennsylvania 16802

Received February 14, 1994<sup>Ⓞ</sup>

**Abstract:** Quantum mechanical (semiempirical) and force field calculations of oligomers of recently reported polycarbyne network backbone polymers indicate that calculated bond lengths between adjacent carbon backbone atoms are elongated relative to the bond distance of a C–C single bond. Some degree of bond cleavage is theorized to occur between adjacent carbon atoms of the polymers' network backbones, resulting in the formation of biradicals. This theory is supported experimentally by the polymers' electronic absorption spectra, their degrees of polymerization, and their ESR spectra, which show a decreasing signal as the steric bulk between adjacent carbons is decreased.

## Introduction

The synthesis of the first member of a new class of carbon-based polymers, poly(phenylcarbyne) ( $[\text{PhC}]_n$ , **1**), has recently been reported.<sup>1,2</sup> This polymer's stoichiometry is identical to that of poly(diphenylacetylene)<sup>3</sup> yet its structure is significantly different. Unlike the polyacetylenes, which are linear polymers whose backbones consist of alternating single and double bonds, poly(phenylcarbyne) has a random network backbone which consists of  $\text{sp}^3$ -hybridized carbon atoms bonded via carbon–carbon single bonds to three other backbone atoms and one phenyl substituent. This backbone structure is unique in carbon-based polymers and has been found to confer novel properties and reactivity on **1**, as, for example, pyrolytic conversion to diamond or diamondlike carbon at atmospheric pressures.<sup>1</sup> Although the network backbone microstructure of poly(phenylcarbyne) and its Group 14 congeners<sup>1,2,4</sup> has been confirmed by  $^{13}\text{C}$  and  $^{29}\text{Si}$  NMR, the macrostructures of this class of polymers have not been established. The seemingly completely random assembly of the polymer backbones defeats any spectroscopic or diffraction characterization technique, since no two polymer molecules in a given sample may display identical macrostructures and therefore no one macrostructure gives rise to enough characteristic signal to be unequivocally detected. Information about the macrostructure of the polymers is becoming increasingly important, however, as polymer macrostructure appears to influence the materials' properties (see below). We have therefore used molecular modeling techniques to provide insights into possible macrostructures for the polycarbyne class of network backbone polymers and to establish what effects varying the steric size of the polymers' substituents may have on preferred macrostructures. Herein we report an

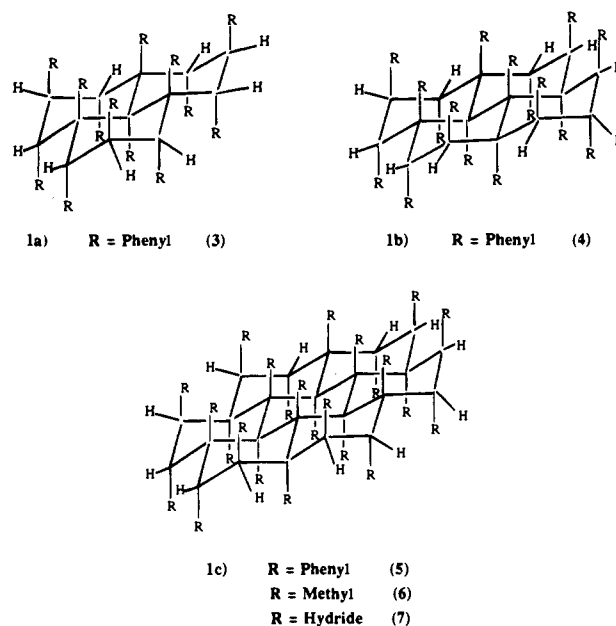


**Figure 1.** Schematic representing models that were created for semiempirical and force field calculations. The models consist of fused, regular, six-membered rings. Smaller networks containing three and four fused rings which are substituted with Ph (**3** and **4**) are shown in parts a and b, respectively. Part c represents larger networks (seven fused rings) which were created that contain Ph (**5**), Me (**6**), and H (**7**) as network substituents.

examination of the structural characteristics of poly(phenylcarbyne) and related network carbyne polymers using both quantum mechanical (semiempirical) and force field calculations. We also report ESR studies on these carbyne polymers which supply further insight into the structural characteristics of this class of materials.

## Experimental Section

**Molecular Dynamic (MD) Simulations.** The MD simulations were carried out using the all-atom AMBER force field.<sup>5</sup> The simulations were done in the gas phase at a constant temperature (300 K)<sup>6</sup> with a 1.0 fs time step. All nonbonded interactions within the molecule were considered. The atomic charges for the molecule were obtained by

(5) Weiner, S. J.; Kollman, P. A.; Nguyen, D. T.; Case, D. A. *J. Comput. Chem.* **1986**, *7*, 230–252.

(6) Berendsen, H. J. C.; Potsma, J. P. M.; van Gunsteren, W. F.; DiNola, A. D.; Haak, J. R. *J. Chem. Phys.* **1984**, *81*, 3684–3690.

(7) Merz, K. M., Jr.; Besler, B. H. *QCPE Bull.* **1990**, *10*, 15.

<sup>Ⓞ</sup> Abstract published in *Advance ACS Abstracts*, August 15, 1995.

(1) Visscher, G. T.; Nesting, D. C.; Badding, J. V.; Bianconi, P. A. *Science* **1993**, *260*, 1496–1499.

(2) Visscher, G. T.; Bianconi, P. A. *J. Am. Chem. Soc.* **1993**, *116*, 1805–1811.

(3) (a) Masuda, T.; Kawai, H.; Ohtori, T.; Higashimuri, T. *Polym. J.* **1979**, *11*, 813–818. (b) Niki, A.; Masuda, T.; Higashimura, T. *J. Polym. Sci., Polym. Chem. Ed.* **1987**, *25*, 1553–1562.

(4) (a) Bianconi, P. A.; Weidman, T. W. *J. Am. Chem. Soc.* **1988**, *110*, 2342–2344. (b) Bianconi, P. A.; Schilling, F. C.; Weidman, T. W. *Macromolecules* **1989**, *22*, 1697–1704. (c) Weidman, T. W.; Bianconi, P. A.; Kwock, E. W. *Ultrasonics* **1990**, *28*, 310–315. (d) Furukawa, K.; Fujino, M.; Matsumoto, M. *Macromolecules* **1990**, *23*, 3423–3426. (e) Bianconi, P. A.; Weidman, T. W.; Kwock, E. W. In *Polymers For Lightwave and Integrated Optics: Technology and Applications*; Hornak, L., Ed.; Optical Engineering Series; Marcell Decker: New York, 1991; pp 195–207. (f) Szymanski, W. J.; Visscher, G. T.; Bianconi, P. A. *Macromolecules* **1993**, *26*, 869–871.

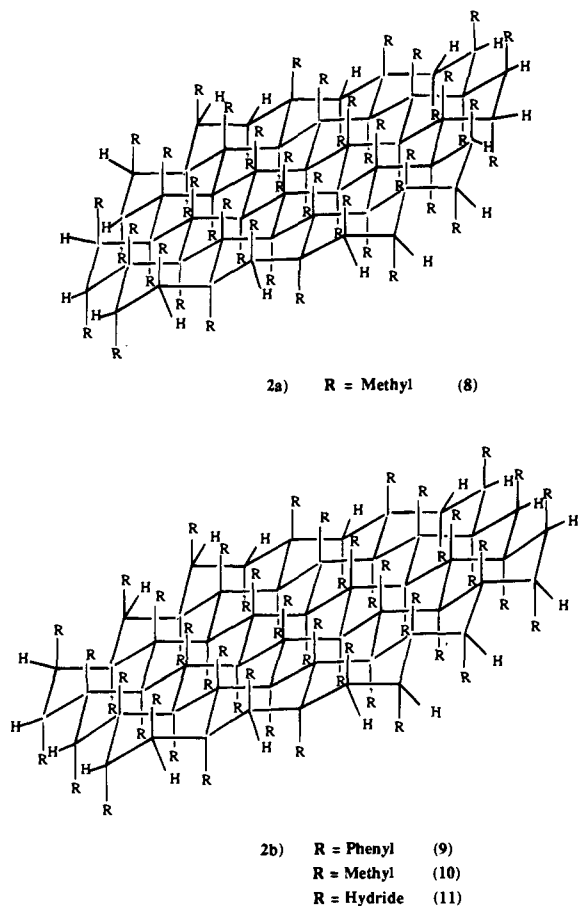


**Figure 2.** Schematic representing larger models that were created for MD simulations and semiempirical calculations. These models also consist of fused, regular six-membered rings. Part a contains seventeen fused rings and is substituted with Me (8). Part b represents larger networks which were created that contain Ph (9), Me (10), and H (11) as network substituents (these models were too large for semiempirical calculations and therefore only MD simulations were examined).

using the electrostatic potential charges calculated from MOPAC 5.0<sup>7</sup> using the MNDO Hamiltonian<sup>8</sup> and electrostatic fitting.<sup>9</sup> A distance-dependent dielectric function was used for all simulations to mimic the effect of solvent. Initially, the structures were minimized for 2000 steps using both steepest decent and conjugate gradient methods. The simulations were run for a total of 160 ps (60 ps equilibration, 100 ps sampling), except for the larger substituted model networks (9–15) which were run for 200 ps (100 ps equilibration, 100 ps sampling). These larger networks (9–15) were equilibrated for 100 ps rather than 60 ps due to the increase in the size of the network. Both poly(phenylcarbyne) (1) and poly(methylcarbyne) (2) have been experimentally synthesized<sup>1,2</sup> and serve as starting structures in this study. Poly(phenylcarbyne) (1) was represented by small network models 3–5 and larger network models 9 and 12–15. Model networks were also constructed for poly(methylcarbyne) (2). These were represented as network models 6, 8, and 10 while the parent carbyne [HC]<sub>n</sub> was represented as models 7 and 11, respectively. All of these models are depicted in Figures 1–4.

**Quantum Mechanics.** Semiempirical calculations were carried out using MOPAC 5.0.<sup>7</sup> The geometries of the structures were optimized using a restricted Hartree–Fock (HF) calculation and the AM1 Hamiltonian.<sup>10</sup> These calculations were limited in the number of atoms which could be explicitly treated due to memory constraints on the computers used. Therefore, only smaller network models were studied using the semiempirical calculations. The systems studied here were

(8) Dewar, M. J. S.; Thiel, W. *J. Am. Chem. Soc.* **1977**, *99*, 4899–4907.

(9) Besler, B. H.; Merz, K. M. J.; Kollman, P. A. *J. Comput. Chem.* **1990**, *11*, 431–439.

(10) Dewar, M. J. S.; Zoebisch, E. G.; Healy, E. F.; Stewart, J. J. P. *J. Am. Chem. Soc.* **1985**, *107*, 3902–3909.

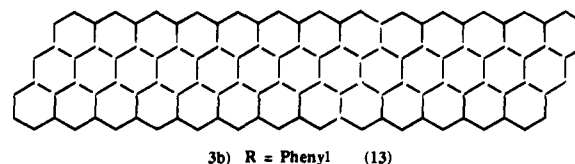
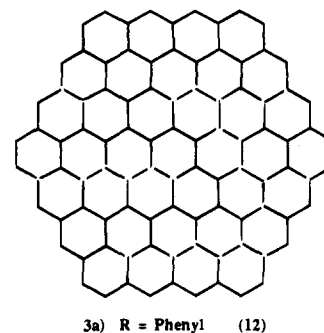


**Figure 3.** Schematic representing the backbones of larger phenyl substituted model networks which consist of fused, regular, six-membered rings. The sizes and shapes of these model networks were varied and represented as concentric structure 12 and sheet-like structure 13 as illustrated in parts a and b, respectively.

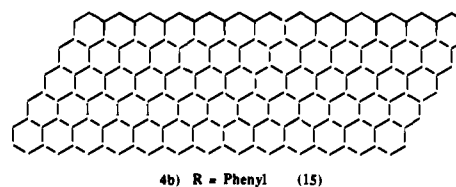
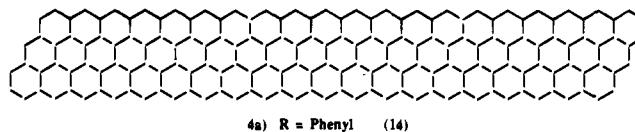


**Figure 4.** Schematic representing large phenyl substituted model networks which consist of regular, fused, six-membered rings. These structures' molecular weights are similar to that of the experimentally synthesized poly(phenylcarbyne) (1) (part a contains 60 repeat units while part b contains 65 repeat units). The sizes and shapes of these structures were varied as well with sheet-like structures 14 and 15 represented in parts a and b, respectively.

networks 3 and 4 for poly(phenylcarbyne) and 6 and 8 for poly(methylcarbyne).

**ESR Spectroscopy.** Poly(phenylcarbyne) (1), poly(methylcarbyne) (2), 99:1 poly(phenyl-*co*-hydridocarbyne) (16), and poly(phenylsilyne) (17) were synthesized as previously reported.<sup>1,2,11</sup> ESR spectra were measured at room temperature for each polymer on solid samples using a Bruker 200 spectrometer operating at 9.70 GHz with a modulation frequency set at 100.0 kHz. Equal amounts of polymer were measured for each sample. In order to quantify the number of unpaired spins present within the samples, each sample was compared to a Bruker weak pitch standard.<sup>12</sup> In quantifying the number of unpaired spins, ratios between each sample were calculated with an uncertainty of approximately 10%.

## Results/Discussion

**MD Simulations.** We have examined models of three different polymers, poly(phenylcarbyne) [PhC]<sub>n</sub> (1), poly(methylcarbyne) [MeC]<sub>n</sub> (2), and the parent polycarbyne [HC]<sub>n</sub> (7). Two of these polymers, 1 and 2, have been experimentally synthesized;<sup>1,2</sup> polycarbyne exists only as a model and was

(11) Bianconi, P. A.; Smith, D. A.; Freed, C. A. *Chem. Mater.* **1993**, *5*, 245–247.

(12) Hyde, J. F. In *Sixth Annual NMR/EPR Workshop*; Palo Alto, CA, 1962.

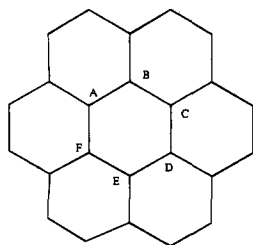


**Figure 5.** Schematic illustrating the determination of average bond lengths and torsion angles within the model networks.

created in order to have a reference for comparative purposes. Although the synthesized polymer networks consist of randomly assembled fused rings of varying sizes, we chose to adopt more simplistic, ordered models for our MD simulations. The models that were chosen consisted of networks of varying numbers of fused, regular, six-membered rings (Figures 1–4). The sizes of the model structures were varied by changing the number of fused cyclohexyl rings contained within the backbone of the network. Smaller phenyl substituted networks (3 and 4) were initially studied while networks containing seven fused rings substituted with Ph (5), Me (6), and H (7) (Figure 1c) also were examined. Larger models containing nineteen fused rings substituted with Ph (9), Me (10), and H (11) were constructed (Figure 2b) as well as model structures substituted with Ph (12–15) (Figures 3 and 4) whose molecular weights are thought to approach that of the actual network polymer, poly(phenylcarbyne) (1) (the number average molecular weight,  $\bar{M}_n$ , for this polymer being 3007 daltons).<sup>1,2,13</sup> As illustrated in Figures 1 and 2, in these network models, 3–11, the substituents of the polymer networks are arranged in alternating axial positions, while the edges of the networks are constructed so that each carbon backbone atom is bonded to two other carbon backbone atoms, one polymer substituent, and one hydrogen atom (this is not illustrated in Figures 3 and 4, however model networks 12–15 were constructed in an identical manner). Although most of the models are oligomers and are not as large as the experimentally synthesized polymers, the models should provide insight into the structural arrangements which are possible in the actual polymer materials.

Structural features of the oligomeric models 3–15 were analyzed by calculating average bond lengths and torsion angles. The averages take into account the symmetry found in the inner portion of the networks: all carbon backbone atoms which were located in the inner portions of the networks are bonded via carbon–carbon single bonds to three other carbon backbone atoms and one polymer substituent, thus making every carbon backbone atom equivalent in the central portion of the network. For example, the C–C bond distances of the inner cyclohexyl rings in 5–7 were calculated by taking the averages of the six individual bond lengths (atoms A–F) which define the ring (Figure 5). Other symmetry-related structural features such as torsion angles within the polymer backbone were also calculated by taking averages of individual torsion angles (for example, in Figure 5 the torsion angles consist of four consecutive carbon backbone atoms, e.g. torsion angle made by atoms A–B–C–D). Average C–C bond lengths and torsion angles (torsion

angles were measured only for the interior portions of the networks) for model networks 3–15 which were obtained from these calculations are shown in Tables 1 and 2. Although model networks 12–15 are much larger, average torsion angles and bond distances were calculated in the same manner due to the symmetry that remains in the interior portions of the model networks.

For the larger network models whose backbones contain nineteen fused rings (9–11), the molecular dynamics simulations indicate that as the size of the polymer backbone substituent increases from hydrogen for polycarbyne (11) to the network with the larger phenyl substituents (9), the distances between adjacent carbon backbone atoms increase by approximately 0.4 Å (Table 1). Conversely, the torsion angles (Table 2) within these larger networks decrease with increasing size of the substituent (smaller network models 5–7 also exhibit this trend and are discussed below). The larger polycarbyne model 11 has an average torsion angle of 58.6°, which is approximately equal to that found in the most stable chair conformation of cyclohexane.<sup>14</sup> Poly(methylcarbyne) has a much lower torsion angle of 37.1° with its backbone showing more planar character. However, the larger poly(phenylcarbyne) model 9 is far more planar (22.9°) and its component cyclohexyl rings deviate significantly from the chair conformation.

The observed increases in bond lengths and decreases in torsion angles within the backbones of 9 are due to both steric and possibly electronic (see below) factors. The large phenyl substituents in 9 cause the amount of steric strain in the network to increase. Visual inspection of our model network reveals that the phenyl rings of 9 are tightly packed due to the constraints on the bond distances between carbon backbone atoms (see Figure 6). Because the phenyl substituents are in close proximity to one another, repulsive van der Waals interactions arise and cause an increase in the amount of steric strain within the polymer backbone. The increase in length of the average carbon–carbon bond distances in the network backbone is attributed to this steric strain.

The methyl substituents of 10 are much smaller than the phenyl substituents of 9. As is shown in Table 1, the average bond distances between adjacent carbon backbone atoms for 10 are less than those calculated for 9. This decrease in bond length is attributed to the steric signature of the polymer substituents. Because the methyl groups of 10 are much smaller than the phenyl substituents of 9, they do not require as large a separation between adjacent substituents to relieve the repulsive interactions and minimize the steric strain experienced by the polymer backbone. Hence, smaller average bond distances and larger torsion angles for the carbon backbone are observed. The same argument holds for the polycarbyne model (11) as well.

The smaller networks 5–7 also give evidence for the steric strain that is present in these network structures. The average bond distances for the inner portions of the networks increase with the size of their network substituents, 5 > 6 > 7 (Table 1). An examination of the torsion angles of the smaller model networks 5–7 reveals the same trend as was seen for the larger model networks 9–11. The polycarbyne model 7 has an average torsion angle of 58.5° while polymer models 5 and 6 have average angles of 21.9° and 34.0°, respectively. The data indicate that the network backbone is becoming increasingly planar as the network substituents become larger and the steric strain in the network increases. The smaller torsion angle for 5 again arises from steric interaction between the phenyl substituents.

(13) GPC molecular weights reported were determined using linear polystyrene standards. Therefore, the absolute molecular weight is probably an underestimation and should only be regarded as a lower limit. The molecular weights determined by GPC for polysilyne network polymers have been found to be underestimated by approximately a factor of 4 through light-scattering techniques.<sup>4,24</sup> Therefore, the polycarbynes molecular weight was approximated analogously by a factor of 4 (the  $\bar{M}_n$  being approximately 3 000 to 12 000 daltons). Hence, the model networks used in our simulations fall within the approximation and should provide a good representation of the network polymer.

(14) Carey, F. A.; Sundberg, R. J. *Advanced Organic Chemistry Part A: Structure and Function*, 3rd ed.; Plenum Press: New York, 1990; pp 802.

**Table 1.** Average C–C Bond Distances for Network Models 3–7

oligomer model	no. of rings in network	C–C dist. <sup>a</sup> (Å)	std dev	C–C dist. <sup>b</sup>	std dev	C–R dist. (Å)	std dev
poly(phenylcarbyne) (3)	3	1.67	0.02	1.59	0.01	1.62	0.01
poly(phenylcarbyne) (4)	4	1.69	0.01	1.61	0.01	1.61	0.01
poly(phenylcarbyne) (5)	7	1.79	0.01	1.65	0.01	1.64	0.01
poly(methylcarbyne) (6)	7	1.64	0.01	1.59	0.01	1.54	0.01
polycarbyne (7)	7	1.54	0.01	1.53	0.01	1.09	0.01
poly(methylcarbyne) (8)	17	1.69	0.01	1.61	0.01	1.56	0.01
poly(phenylcarbyne) (9)	19	1.96	0.01	1.73	0.004	1.65	0.01
poly(methylcarbyne) (10)	19	1.69	0.01	1.63	0.01	1.55	0.01
polycarbyne (11)	19	1.54	0.01	1.53	0.01	1.09	0.01
poly(phenylcarbyne) (12)	37	2.10	0.003	1.80	0.003	1.57	0.01
poly(phenylcarbyne) (13)	39	1.95	0.002	1.80	0.002	1.70	0.004
poly(phenylcarbyne) (14)	60	1.96	0.002	1.82	0.002	1.62	0.003
poly(phenylcarbyne) (15)	65	2.10	0.003	1.89	0.004	1.60	0.005

<sup>a</sup> Distances between carbon backbone atoms in the inner portion of the networks. <sup>b</sup> Distances between carbon backbone atoms on the edges of the networks.

**Table 2.** Average Torsion Angles for Interior Network Backbone Atoms

oligomer model <sup>a</sup>	no. of rings in network	torsion angle (deg)	std dev
poly(phenylcarbyne) (5)	7	21.8	2.2
poly(methylcarbyne) (6)	7	34.0	2.7
polycarbyne (7)	7	58.5	2.7
poly(methylcarbyne) (8)	17	38.1	1.4
poly(phenylcarbyne) (9)	19	22.9	1.9
poly(methylcarbyne) (10)	19	37.1	1.3
polycarbyne (11)	19	58.6	2.2
poly(phenylcarbyne) (12)	37	26.6	0.8
poly(phenylcarbyne) (13)	39	32.9	0.6
poly(phenylcarbyne) (14)	60	32.7	0.5
poly(phenylcarbyne) (15)	65	27.7	0.7

<sup>a</sup> Torsion angles were not measured for models 3 and 4 because they did not contain an interior cyclohexyl ring.

The degree of crowding between polymer substituents within the various network models can be assessed by an examination of the outer portion of the networks as well. The calculated average bond length between adjacent carbon backbone atoms on the edge of the network of **9** is 1.73 Å (Table 2). This bond length is less than those calculated for the inner fused rings of the network of **9** (1.96 Å), yet still greater than the average bond lengths for both the inner and edge backbone distances calculated for **10** and **11**, the methyl- and hydrogen-substituted model networks (1.68 and 1.54 Å, respectively). The edge carbon atoms of the backbone of **5** and **9** [R<sub>2</sub>CHPh] have one less linkage to the network backbone than do the inner network atoms. There are two substituents (a phenyl ring and a hydrogen atom) for the edge carbon backbone atom rather than just the one phenyl substituent found in the inner portion of the network. Visual inspection shows the phenyl rings are not as tightly packed along the edges of the network (see Figure 6). Because of the orientation of the substituents, a decrease in the steric strain at the edges of the networks is expected. This is attributed to both the decrease in linkages to the network backbone and the presence of the smaller hydrogen atoms. Consequently the steric strain introduced by the network substituents at the edges is reduced to some degree, as evidenced by the reduction in the C–C bond lengths when compared to the inner portion of the network backbone.

This trend of bond length reduction at the edges of the network backbone also exists for the smaller models **5** and **6**. This supports our conclusion that the degree of crowding associated with the network substituents is proportional to the amount of steric strain present within the network and hence

contributes to the preferred conformations of our models. Increase in steric strain with increasing substituent size has also been observed in substituted dodecahedranes, which can be regarded as oligomers of the polycarbynes.<sup>15</sup>

The  $\pi$ -stacking adopted by phenyl rings may also contribute to the conformations of the backbones of network models **3–5**, **9**, and **12–15**. The strong attraction or repulsion associated with  $\pi$ -systems has been shown to determine the conformational preference and binding properties of polyaromatic macrocycles.<sup>16</sup> The most important interactions between such  $\pi$ -systems are quadrupole–quadrupole electrostatic interactions.<sup>17</sup> For aromatic rings with nonpolar substituents,  $\pi$ – $\pi$  electronic repulsions will dominate if the aromatic rings are arranged in a stacked or face-to-face geometry. Conversely, if the substituents are arranged in a T-structure (phenyl rings arranged so that the edge of one ring is perpendicular to the face of a second ring), electronic attraction of the  $\pi$ – $\sigma$  type will dominate (see Figure 9 of ref 18).<sup>18</sup> Phenyl rings will therefore try to orient themselves in a tilted T-structure in order to achieve the lowest possible interaction energy between them.<sup>18,19</sup> An examination of stacked and perpendicular arrangements of  $\pi$ -systems showed that the perpendicular arrangement displays the lower free energy due to the more favorable  $\pi$ – $\sigma$  interactions.<sup>20</sup> For our model systems **3–5**, **9**, and **12–15**, visual inspection reveals that adjacent phenyl substituents are tightly packed in an orientation intermediate between the stacked and T-conformations (see Figure 6), presumably resulting in unfavorable, repulsive van der Waals interactions between them. Dial plots of the phenyl substituted model networks were constructed (data not shown) that indicate that the phenyl rings do not undergo facile rotations along the C(sp<sup>3</sup>)–C(sp<sup>2</sup>) (C<sub>backbone</sub>–C<sub>phenyl</sub>) bond. The phenyl substituents are tightly packed and as expected do not move significantly from their positions on the network backbones of the polymer. Hence, the arrangement of the phenyl substituents contributes significantly to the calculated structural parameters which are indicated by our models.

Our MD simulations also indicate a difference in the average bond lengths between the backbone carbon atoms for the inner portions between the smaller and larger networks for both the phenyl and methyl substituted network models (Table 1), which

(16) (a) Hunter, C. A.; Meah, N. M.; Sanders, J. K. M. *J. Am. Chem. Soc.* **1990**, *112*, 5773–5780. (b) Anderson, H. L.; Hunter, C. A.; Meah, N. M.; Sanders, J. K. M. *J. Am. Chem. Soc.* **1990**, *112*, 5780–5789. (c) Hunter, C. A.; Leighton, P.; Sanders, J. K. M. *J. Chem. Soc., Perkin Trans. 1* **1989**, 547–552.

(17) Linse, P. *J. Am. Chem. Soc.* **1992**, *114*, 4366–4373.

(18) Hunter, C. A.; Sanders, J. K. M. *J. Am. Chem. Soc.* **1990**, *112*, 5525–5534.

(19) Jorgensen, W. L.; Severance, D. L. *J. Am. Chem. Soc.* **1990**, *112*, 4768–4774.

(20) Linse, P. *J. Am. Chem. Soc.* **1993**, *115*, 8793–8797.

(15) Wahl, F.; Wörth, J.; Prinzbach, H. *Angew. Chem.* **1993**, *32*, 1722–1726.

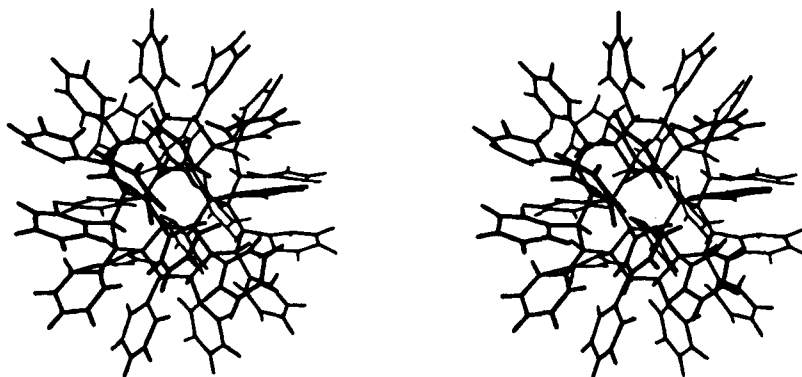


Figure 6. Stereo view of model network 5 illustrating the packing arrangement of its phenyl substituents.

may be indicative of an important structural feature of the polycarbyne polymer models. For the inner portion of the poly(phenylcarbyne) networks, the average bond distance between the backbone carbons of **5** is 1.79 Å, while that of **9** is significantly longer, 1.96 Å. The poly(methylcarbyne) network exhibits the same trend as the average bond distance between adjacent carbon backbone atoms of **6** is 1.64 Å, while that of **10** is larger, 1.69 Å. This difference is attributed to the sizes of the backbone networks of the two models. The network backbone of poly(phenylcarbyne) (**1**) is much larger than those of our model networks.<sup>1,2</sup> Because of the size of **1**, the number of carbon backbone atoms located along the edge of the polymer is small as compared to those of the inner portion of the network. Hence, the inner portion of the polymer will have a greater effect on the physical properties of **1** than will the edge of the network. Due to its larger inner network, **9** and **10** are thought to be better representations of the actual network backbone structures of poly(phenylcarbyne) (**1**) and poly(methylcarbyne) (**2**) than are **5** and **6**. However, **9** and **10** are still not as large as the actual carbyne network polymers. Therefore, larger model networks were constructed that have molecular weights which approach that of the actual network polymer, poly(phenylcarbyne) (**1**) (the  $M_n$  was found to be 3007 daltons for poly(phenylcarbyne) (**1**)).<sup>1,2,13</sup>

For comparison to our smaller phenyl substituted networks, structures with phenyl substituents were created that have an increased number of repeat units. The backbones of these four model networks (**12**–**15**) were arranged into two distinct orientations (Figures 3 and 4). Model network **12** was constructed so that the backbone formed a concentric structure around an innermost ring (see Figure 3a). The average calculated bond length between adjacent carbon backbone atoms for the interior of the network of **12** is 2.10 Å (Table 1). This bond distance is greater than those previously calculated for phenyl substituted model networks (**5** and **9**) and indicates that for concentric structures, increasing the size of the model network may also result in an increase in the amount of strain within the system. The smaller average torsion angle (26.6°) calculated for this system supports this finding as well. In order to more closely examine this phenomenon, model networks were constructed which consisted of sheets of fused, regular, six-membered rings, **13** and **14** (Figures 3b and 4a), rather than the previously studied concentric structures. Average bond lengths of 1.95 and 1.96 Å were calculated for **13** and **14**, respectively (Table 1). These bond distances were found to be equal in magnitude when compared with our smaller network model **9**. Average torsion angles of 32.9° and 32.7° were calculated respectively for model networks **13** and **14** and also indicate that there is some degree of strain within these networks. The backbone of the final model network, **15**, resembled more of a concentric structure (Figure 4b). An average bond length of

2.10 Å (Table 1) was calculated for this structure with a torsion angle of 27.7° (Table 2). Model networks **14** and **15** have approximately the same molecular weights that are thought to exist for the actual polymer (**1**),<sup>1,2,13</sup> and it appears that these model networks are good representations for the polymer system. In both **14** and **15**, the increases in the bond lengths and the flattening of the carbon backbones of these larger model networks as compared to unsubstituted model network **7** indicate that there is some degree of strain in these systems.

In examining the data of the four larger network structures, **12**–**15**, both similarities as well as some notable differences were found to exist. As expected, there is some degree of strain present in all of the model networks. The elongation of the C–C backbone distances in our models as compared to a C–C single bond (1.54 Å)<sup>21</sup> indicates strain in the network backbone resulting from unfavorable steric interactions between the polymer substituents. The average torsion angles calculated for these models illustrate that the backbones for these phenyl substituted models are becoming increasingly planar and thus confirming the strain predicted by the increase in the bond distances between C–C backbone atoms. However, upon closer examination, differences in the magnitude of the bond distances and torsion angles exist between the “sheet-like” structures (**13** and **14**) and the “concentric” structures (**12** and **15**). It would appear that structures **12** and **15** adopt a more highly strained conformation than structures **13** and **14**. This hypothesis is based on the larger bond distances and the smaller torsion angles of **12** and **15** which indicate a highly strained system. These results indicate that sheets of fused ring systems similar to model networks **13** and **14** may be the preferred conformation for the poly(phenylcarbyne) network polymer. However, it is thought that the experimentally synthesized poly(phenylcarbyne) (**1**) does not consist entirely of fused, regular, six-membered rings and that there is some degree of randomness associated with the polymer network backbone. Incorporating rings of various sizes within the polymer network backbone may alleviate some of the bad steric interactions of the polymers’ side chain substituents which could result in alternative conformations. The formation of biradicals in the polymer backbone may also alleviate bad steric interactions as well due to the possible bond cleavage that may be occurring in the polymer backbone. This could result in a different preferred conformation other than the structure predicted by our simulations. Nonetheless, it appears that a sheet structure will have a lower strain energy than a concentric structure regardless of the randomness of the ring sizes. Thus we predict that the synthesized polymers probably will adopt a sheet structure.

The 1.96 Å average distance between adjacent carbon atoms in the inner backbone of **9** is quite long for C–C single bonds,

(21) Greenwood, N. N.; Earnshaw, A. *Chemistry Of The Elements*; Pergamon Press: New York, 1984; pp (a) 296–385, (b) 306.

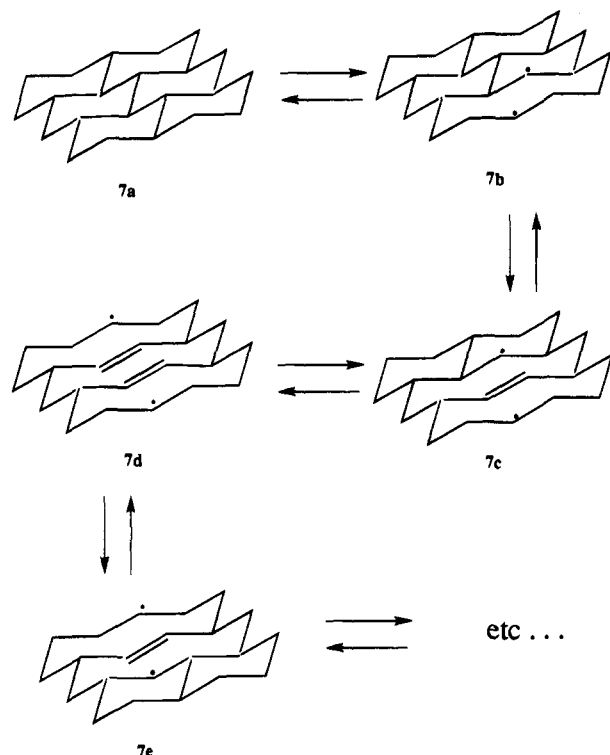


**Figure 7.** Schematic representing the possible bond cleavage and radical formation within polycarbyne backbones.

and arises from the inability of the potential function used in the MD simulations to mimic bond breaking. The long average bond length calculated for **9** suggests that some degree of bond breaking may occur within the backbone of polycarbynes, resulting in the formation of biradicals. Bond cleavage within the polymer backbone would allow for maximum separation between adjacent substituents and would therefore lower the repulsive van der Waals interactions between them. It should therefore relieve steric strain and allow for more favorable backbone conformations by alleviating the crowding generated by neighboring phenyl substituents. Figure 7 illustrates schematically the bond cleavage which is proposed to occur in the backbones of polycarbynes. The bond cleavage produces biradicals which may rearrange to create areas of unsaturation within the polymer backbones. This process may occur throughout the polymer's backbones, resulting in some radical mobility. This bonding model for the backbones of polycarbynes is analogous to that proposed for amorphous silicon and germanium solid-state structures based on continuous random network models, in which some atoms are only three-coordinate and are left with a single electron in a "dangling bond".<sup>22</sup>

**Quantum Mechanical Calculations.** Because of the structural characteristics and the large amount of strain predicted by our MD simulations as well as the inability of the classical force field to mimic bond breaking, it was decided to examine the carbyne polymers using a quantum mechanical potential. AM1 calculations were carried out on model structures in order to examine the preferred geometries of the model structures and to also see if the strain that was predicted by MD simulations was also present in these calculations as well. As mentioned previously, smaller models as compared to those used in the MD simulations were used for the calculations due to computer memory constraints. Like the MD simulations, the models that were chosen consisted of networks of varying numbers of fused, regular, six-membered rings (Figures 1 and 2). Model networks

**Table 3.** Average C–C Bond Distances and Torsion Angles for Network Models **3**, **4**, **6**, and **8**

oligomer model	no. of rings in network	C–C dist. <sup>a</sup> (Å)	std dev	C–C dist. <sup>b</sup>	std dev	torsion angle <sup>c</sup> (deg)	std dev
poly(phenylcarbyne) ( <b>3</b> )	3	1.62	0.01	1.57	0.03		
poly(phenylcarbyne) ( <b>4</b> )	4	1.65	0.03	1.57	0.03		
poly(methylcarbyne) ( <b>6</b> )	7	1.60	0.01	1.57	0.01	43.5	4.4
poly(methylcarbyne) ( <b>8</b> )	17	1.66	0.02	1.59	0.02	47.4	0.5

<sup>a</sup> Distances between carbon backbone atoms in the inner portion of the networks. <sup>b</sup> Distances between carbon backbone atoms on the edges of the networks. <sup>c</sup> Torsion Angles for atoms in the inner portion of the polymer networks. Models **3** and **4** do not contain an inner ring to calculate the desired torsion angles.

substituted with Ph (**3** and **4**) consisted of three and four fused rings, respectively (Figures 1a and 1b). Larger networks substituted with Me (**6** and **8**) containing seven and seventeen fused rings were also studied (Figures 1c and 2a). The models were constructed in an identical manner as those used in the MD simulations with substituents alternating axial positions. Although the phenyl substituted model networks **3** and **4** are much smaller than those used in the MD simulations, they still should provide some insight into structural characteristics of the carbyne polymer.

Structural features of the oligomeric models (**3**, **4**, **6**, and **8**) were evaluated after optimizing the systems' geometries. Because of the symmetry associated with our models, averages were again calculated for both bond lengths and torsion angles in each model network. For example, the three interior bond lengths were averaged and considered to be equivalent in model network **3**. Torsion angles within the polymer backbone were also calculated by taking averages of individual torsion angles. (The same procedure was used in calculating torsion angles and bond lengths for the MD simulations.) Average C–C bond lengths and torsion angles for model networks **3**, **4**, **6**, and **8** are shown in Table 3.

For the phenyl substituted network models whose backbones contain three and four fused rings (**3** and **4**), the AM1 calculations are in agreement with the MD simulations. A lengthening of the distances between adjacent carbon backbone atoms is evident for both **3** and **4**. The smaller model network **3** has an average bond length of 1.62 Å while that of **4** has increased slightly to 1.65 Å. As previously stated, the phenyls are tightly packed due to constraints on the bond distances between the carbon atoms in the network backbone. Hence, an increase in steric strain resulting from the close proximity of the phenyl substituents causes the lengthening of the bond distances in the network backbone.

Results of the methyl substituted models (**6** and **8**) are similar to those of models **3** and **4**. The AM1 calculations also indicate a lengthening of the distances in the network backbone as compared to a standard C–C single bond (1.60 and 1.65 Å for **6** and **8**, respectively). Although the lengthening of the bond distances in the network backbone for **6** and **8** is not as large as seen for the phenyl substituted network models **3** and **4**, the calculations support previous findings that an increase in steric size of network substituents results in steric strain within the polymer networks. Thus, this increased strain in the polymer networks causes the backbone bond distances to elongate and may give rise to some degree of bond breaking within the backbone of polycarbynes, resulting in the formation of biradicals.

An examination of the calculated torsion angles for our network models supports the theory of increasing strain with increasing size of the polymer substituents. The network substituents cause the backbone to become increasingly planar

as the steric signature of these substituents increases. The torsion angles for the phenyl substituted network models (**3** and **4**) were not measured due to the absence of a central fused ring, however visual inspection of the two models revealed increased planarity in the network backbone. Methyl substituted oligomeric models **6** and **8** have average torsion angles of  $43.5^\circ$  and  $47.4^\circ$ , respectively. These data are again in support of the results obtained from the MD simulations. The network backbone becomes increasingly planar as the sizes of the network substituents become larger and the steric strain in the network increases.

Both force field and semiempirical calculations were performed on phenyl and methyl substituted networks in order to compare their results since semiempirical calculations give a more realistic representation of stretched C–C bonds than do the force field based MD simulations. An examination of the results illustrates that the same trends exist for both the semiempirical and the force field calculations. The average bond lengths for the AM1 calculations were found to be slightly less than those calculated from the MD simulations (Tables 1 and 3). However, the bonds' elongations still suggest that steric strain is present within the polymer network and is responsible for the bond lengthening in the network backbone. Torsion angles that were calculated from the AM1 optimized geometries are slightly greater than those calculated for the MD simulations. Even though the angle is greater for the AM1 calculations, there still remains a large decrease from the  $60^\circ$  torsion angle found in unsubstituted cyclohexane. This decrease in the torsion angle supports the strain theory based on our previous MD simulations. Although there are differences between the force field and semiempirical calculations, the same trends exist and thus support our conclusions. Increasing the steric signature of the polymer substituents results in an increase in the strain found within the polymer backbone.

**ESR Spectroscopy.** Both the force field and semiempirical calculations indicate steric strain that is induced by polymer substituents causes bond elongation and possible bond cleavage in the polymer network backbone. That "steric strain induced" C–C bond cleavage occurs within the backbones of polycarbyne network polymers is supported experimentally by the observation of unpaired electrons in polycarbynes.<sup>2</sup> The experimentally-synthesized polymers poly(phenylcarbyne) (**1**), poly(methylcarbyne) (**2**), and 99:1 poly(phenyl-*co*-hydridocarbyne) (**16**) exhibit ESR signals characteristic of carbon-centered radicals, with *g*-values of 2.0026, 2.0033, and 2.0029, respectively (Figure 8). The ratio of the number of unpaired spins for poly(phenylcarbyne) (**1**) to 99:1 poly(phenyl-*co*-hydridocarbyne) (**16**) is 5.7:1 while that for poly(phenylcarbyne) (**1**) to poly(methylcarbyne) (**2**) is 13.3:1.

Because the polymer backbone is highly rigid, the steric strain in the polymer systems results in bond cleavage and in the formation of biradicals. That radical formation is driven by relief of steric strain caused by the size of the polycarbynes' substituents is demonstrated experimentally by comparison of the ESR spectra of four different experimentally synthesized polymers, poly(phenylcarbyne) (**1**), 99:01 poly(phenyl-*co*-hydridocarbyne) (**16**), poly(methylcarbyne) (**2**), and poly(phenylsilylyne) (**17**) (Figure 8). The intensities of the ESR absorptions are indicative of the amount of unpaired spins present within the sample. As shown in Figures 8a–8c, the intensity of the ESR signals of these polycarbynes decreases as the size of the polymers' substituents decreases. The number of radicals formed within the polymer is dependent on the size of the backbones' substituents, which our models indicate also induces steric strain within the backbone. According to our

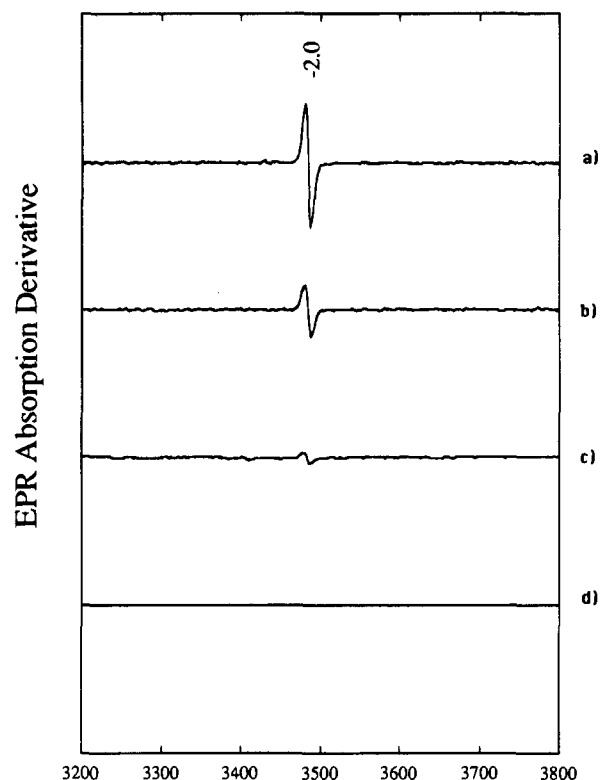


**Figure 8.** ESR spectra of (a) poly(phenylcarbyne) (**1**), (b) poly(phenyl-*co*-hydridocarbyne) (**16**), (c) poly(methylcarbyne) (**2**), and (d) poly(phenylsilylyne) (**17**).

models, the larger phenyl substituents of **1** should induce a large amount of steric strain within the polymer backbone and hence greater radical formation to relieve this strain. The phenyl rings may then stabilize the radicals through delocalization in the phenyl substituent. As the steric size of the substituents on the polycarbyne backbones is decreased, from polymers **16** to **2**, the intensity of the ESR signal also decreases, suggesting, as predicted by our models, that the lesser degree of steric strain experienced by these polymers' backbones is the cause of a lower degree of bond cleavage in the backbone. No ESR signal is seen for the silicon-based congener of **1**, poly(phenylsilylyne) (**17**, Figure 8d). The Si–Si bonds which form this polymer's backbone are much longer than the C–C single bonds which make up the backbone of **1** ( $2.35 \text{ \AA}$  as compared to  $1.54 \text{ \AA}$ ).<sup>21</sup> A silicon-based polymer backbone substituted with phenyl groups therefore would not experience as much crowding as would the identically-substituted carbon-based polymer, and should display little or no biradical formation and ESR signal. These results support the MD simulations by illustrating the relationship between the size of the polymer substituent and the amount of steric strain within the polymer system, as evidenced by the number of biradicals formed by bond cleavage.

The electronic absorption spectra displayed by the polycarbynes<sup>1,2</sup> also support our models' prediction of a strained network backbone structure. These spectra are nearly identical to those of their silicon analogues, the polysilynes,<sup>4</sup> consisting of intense broad absorptions with onset at approximately 450 nm, increasing gradually in intensity with decreasing wavelength to 200 nm. For polysilynes, these absorptions are attributed to Si–Si  $\sigma$ -conjugation over the three-dimensional polymer backbone.<sup>4</sup> Because of the similarity of their electronic spectra to those of polysilynes, the polycarbyne backbones also appear to be  $\sigma$ -conjugated. Such  $\sigma$ -conjugation of C–C bonds is also seen in small molecules which incorporate strain fused rings.<sup>23</sup> The strain which our calculations indicate is present in the fused

rings of the polycarbyne backbones should lower the C–C bond strength and thus the energy of the bonds'  $\sigma$ – $\sigma^*$  transitions from the vacuum UV (where the  $\sigma$ – $\sigma^*$  transition of unstrained C–C bonds occurs<sup>21</sup>) to the observed UV and visible frequencies. The radical transfer mechanism shown in Figure 7 could also contribute to the polycarbynes' low-energy electronic absorptions: delocalization of biradicals through the polycarbynes' backbone as depicted in Figures 7c–7e should also give rise to lower-frequency electronic absorptions, as could defects (for example, OH or Cl terminations) in the polymers' structures.

Our calculations' indication that strain within polycarbyne network backbones, induced by steric crowding of the substituents (see above), increases as the network backbone increases in size suggests that the degree of polymerization which is seen in polycarbynes should decrease as the size of backbone substituents increases. This prediction is also confirmed by the experimental determination of the polycarbynes' molecular weights. The number average molecular weights,  $\bar{M}_n$ , for poly(phenylcarbyne) (1),<sup>1,2</sup> 99:1 poly(phenyl-*co*-hydridocarbyne) (16),<sup>2</sup> poly(methylcarbyne) (2),<sup>2</sup> and poly(phenylsilyne) (17)<sup>11</sup> are 3007, 4168, 4425, and 8775 daltons, respectively. These molecular weights demonstrate that, as was seen for inorganic-backbone network polymers,<sup>4</sup> the degree of polymerization attained by the polycarbynes is proportional to the steric signature of their substituents, suggesting that large substituents can be incorporated only in networks which, by virtue of their smaller sizes, can minimize steric repulsions between substituents.

## Conclusions

Quantum mechanical (semiempirical) calculations and MD simulations of models for a new class of carbon-based polymers, polycarbynes, were carried out in order to provide some insight into this class of polymers' structural characteristics. The models that were used in our simulations consisted of structures whose backbones were constructed of fused, regular, six-membered rings of various sizes and arranged into various conformations. Results of the initial MD simulations on smaller model networks suggest that some degree of bond cleavage occurs within the polymer backbones that is increased by strain induced steric repulsions between the polymers' side chain substituents. Results of MD simulations for larger models which

have molecular weights that approach that of the actual polymer support this proposed bond cleavage as well. Semiempirical studies are in agreement with the MD simulations as results also indicate strain being present in the polymer backbone and also suggest that some degree of bond cleavage may be occurring in the carbon network backbone. These calculations are supported experimentally by the polymers' ESR spectra, electronic spectra, and degrees of polymerization.

Also of note are the differences in the construction of the backbones between the larger model networks. Results indicate that sheets of fused ring systems may be the more favorable configuration for the poly(phenylcarbyne) network polymer rather than a concentric structure. However, our model systems do not incorporate random ring sizes into the polymer backbone and consist entirely of fused, regular, six-membered rings. The incorporation of various ring sizes into the network backbone may alleviate some of the strain induced through bad steric interactions between the polymers' side chain substituents. This may result in less crowding between the polymer substituents and a preferred configuration other than the ideal "sheet-like" structure predicted by our calculations. Another factor which needs to be considered is the possible bond cleavage and biradical formation in the polymer backbone. This also may relieve bad steric interactions as well and result in a conformation other than that predicted by our simulations. Even though our simulations lack randomness in the polymer backbone, it nevertheless appears that a sheet structure will have a lower strain energy than the concentric structure regardless of the ring sizes. Many of the unfavorable steric interactions associated with the polymers' substituents are not present in this sheet structure. Hence, we predict that a sheet structure will be the adopted configuration of the synthesized polymers.

Future investigations will focus on modeling this class of network polymers using both quantum mechanical calculations as well as more sophisticated molecular mechanical methods that are capable of representing bond breakage. These calculations on larger models will give a more realistic representation of the C–C bonds in the polymer network and provide even further insight into the polymers' network backbone.

**Acknowledgment.** We thank Dr. M. Crowder, Dr. P. M. Lanahan, and Jim Yount of the Pennsylvania State University for their assistance in acquiring ESR spectra. P.A.B. is a Beckman Young Investigator (1992–1994) and the recipient of a Camille and Henry Dreyfus Teacher-Scholar Award (1992–1997).

**Supporting Information Available:** Tables of atomic charges for the repeat units used for our models (4 pages). This material is contained in many libraries on microfiche, immediately follows this article in the microfilm version of the journal, can be ordered from the ACS, and can be downloaded from the Internet; see any current masthead page for ordering information and Internet access instructions.

JA9404936

(23) (a) Hush, N. S. et al. *Chem. Phys. Lett.* **1985**, *117*, 8–11. (b) Warman, J. M. et al. *Nature* **1986**, *320*, 615–616. (c) H. Oevering et al. *J. Am. Chem. Soc.* **1987**, *109*, 3258–3269. (d) M. N. Paddon-Row et al. *J. Phys. Chem.* **1988**, *92*, 6958–6962. (e) Verhoeven, J. W. *Pure Appl. Chem.* **1986**, *58*, 1285–1290. (f) Olah, G. A. et al. *J. Am. Chem. Soc.* **1985**, *107*, 2764–2767. (g) Dewar, M. J. S. *J. Am. Chem. Soc.* **1984**, *106*, 669–682. (h) Gleiter, R.; Schafer, W. *Acc. Chem. Res.* **1990**, *23*, 369–375. (i) Paddon-Row, M. N.; Patney, H. K.; Brown, R. S.; Houk, K. N. *J. Am. Chem. Soc.* **1981**, *103*, 5575–5577. (j) Balaji, V.; Jordan, K. D.; Burrow, P. D.; Paddon-Row, M. N.; Patney, H. K. *J. Am. Chem. Soc.* **1982**, *104*, 6849–6851. (k) Surya Prakash, G. K.; Fessner, W.; Olah, G. A.; Lutz, G.; Prinzbach, H. *J. Am. Chem. Soc.* **1989**, *111*, 746–748.

(24) Bianconi, P. A.; Weidman, T. W.; Schilling, F. C. In Polyalkylsilyl-ynes: Synthesis and Properties of "Two-Dimensional" Silicon–Silicon Bonded Network Polymers. *MRS Symp. Proc.* **1991**, *131*, 425–429.